Journal of Molecular Spectroscopy 257 (2009) 82–93

Contents lists available at ScienceDirect

Journal of Molecular Spectroscopy

journal homepage: www.elsevier.com/locate/jms

Microwave spectrum of 1,2-propanediol

F.J. Lovas [a,b,*], D.F. Plusquellic [a], Brooks H. Pate [b], Justin L. Neill [b], Matthew T. Muckle [b], Anthony J. Remijan [b,c]

[a] Optical Technology Division, National Institute of Standards and Technology, Gaithersburg, MD 20899-8441, USA
[b] Center for Chemistry of the Universe, Department of Chemistry, University of Virginia, McCormick Rd., P.O. Box 400319, Charlottesville, VA 22904-4319, USA
[c] National Radio Astronomy Observatory, 520 Edgemont Rd., Charlottesville, VA 22903-2475, USA

ARTICLE INFO

Article history:
Received 2 May 2009
In revised form 5 June 2009
Available online 1 July 2009

Keywords:
Ab initio calculation
Dipole moment
Microwave spectrum
Propanediol
Rotational spectrum
Structure

ABSTRACT

The microwave spectrum of the sugar alcohol 1,2-propanediol ($CH_3CHOHCH_2OH$) has been measured over the frequency range 6.5–25.0 GHz with several pulsed-beam Fourier-transform microwave spectrometers. Seven conformers of 1,2-propanediol have been assigned and ab initio electronic structure calculations of the 10 lowest energy forms have been calculated. Stark effect measurements were carried out on several of the lowest energy conformers to provide accurate determinations of the dipole moment components and assist in conformer assignment.

1. Introduction

Recently, the simplest sugar, glycolaldehyde (CH_2OHCHO) [1], and its diol derivative, ethylene glycol (CH_2OHCH_2OH) [2], were detected towards the interstellar molecular cloud, Sgr B2 (N-LMH). The identification of sugar alcohols and sugar acids in the Murchinson and Murray meteorites [3] has also increased the interest in investigating interstellar sugars and their derivatives in astronomical environments. 1,2-Propanediol is one of two forms of propanediol, the other being 1,3-propanediol, and is related to ethylene glycol by the addition of a methyl group to one of the carbon atoms in place of an H atom. Because of its structural similarity to ethylene glycol, 1,2-propanediol is of interest as a potential interstellar molecule.

1,2-Propanediol is an asymmetric top molecule with numerous low energy conformers. Vázquez et al. [4] reported optimized geometries for 23 conformers from Pulay's gradient optimized ab initio calculations [5] using the 4-21G basis set with eight conformers having relative energies below 560 cm^{-1}. Since this is a rather small basis set, the current ab initio calculations were carried out at the MP2 level [6] with the augmented correlation consistent triple zeta basis set, aug-cc-pVTZ, [7] beginning with the eight lowest energy structures reported in [4]. We use the conformer labeling scheme employed in Ref. [4] as well as their atom numbering for easier comparisons. This labeling scheme provides a three character label, xXx, where X (capital for the OCCO dihedral angle orientation and lower case for the hydroxyl hydrogens) can be G, or G′, depending on the *gauche* position of the atom considered with respect to a reference bond. G and G′ indicate an anticlockwise or a clockwise rotation from the *cis* (*syn*) position of O2–C3–C4–O5 dihedral angle for the X values and similarly for the HOCC dihedral angles represented by x whose values may be g, g′, t, or t′. The first x represents the position of the hydroxyl hydrogen H1 with respect to C4, the second x the position of H6 with respect to C3.

The microwave spectra of two low energy conformers of 1,2-propanediol, labeled as g′Gt (conformer 1 here) and gG′t (conformer 2), were previously investigated in the frequency range from 26.5 to 40 GHz using a conventional Stark-modulated microwave absorption spectrometer [8]. The gG′t (conformer 2) was assigned to be the most stable. We have expanded the data obtained in Ref. [8] by a new series of measurements in the 6.5–25 GHz frequency range using a National Institute of Standards and Technology (NIST) cavity spectrometer and the broadband instrument at University of Virginia. Since seven of the eight low energy conformers were assigned from the surveys, we extended the structure calculations to cover conformers 9 to 12 reported by Vázquez et al. [4]. However, only conformers 9 and 12 were stable forms with conformers 10 and 11 relaxing to other conformer structures.

2. Experimental details

At NIST, measurements were carried out using a Fabry–Perot cavity, pulsed nozzle Fourier-transform microwave (FTMW)

* Corresponding author. Address: Optical Technology Division, National Institute of Standards and Technology, 100 Bureau Drive Mail Stop 8441, Gaithersburg, MD 20899-8441, USA. Fax: +1 301 869 5700.
E-mail address: francis.lovas@nist.gov (F.J. Lovas).

0022-2852/$ - see front matter © 2009 Elsevier Inc. All rights reserved.
doi:10.1016/j.jms.2009.06.013

spectrometer of the Balle–Flygare type [9] designed by Lovas and Suenram [10,11]. This design employs a co-axially oriented nozzle [12] and PC based system for timing, mirror movement, nozzle control, synthesizer tuning and signal processing and uses the FTMW++ software system designed by Grabow [13]. Under ambient conditions, 1,2-propanediol has a very low vapor pressure. Therefore, in order to obtain a sufficient vapor pressure of 1,2-propanediol, the sample was heated up to 60 °C in a nozzle equipped with a reservoir. The jet-cooled expansion was produced by mixing the vapor with a 20% helium and 80% neon by volume carrier gas at a total pressure of 100 kPa (1 bar) and then injecting it into the cavity through 1 mm nozzle orifice along the axis of the Fabry–Perot cavity and parallel to the microwave field. Molecular transitions, observed as Doppler doublets, had line widths of 5 kHz, and the frequency measurement uncertainties were estimated to be 2.5 kHz in most cases.

Measurements at the University of Virginia were performed with a broadband chirped-pulse FTMW spectrometer [14]. The "B" configuration described in Ref. [14] was used with an additional upgrade of the arbitrary waveform generator (AWG) to a 24 Gs/s sample rate (Tektronix AWG7122B) [15]. The chirped microwave excitation pulse was created by mixing a linear sweep pulse generated by the AWG with a 18.95 GHz phase-locked dielectric resonator oscillator (PDRO). The AWG pulse sweeps the frequency range of 12–0.5 GHz with a duration of 1 μs creating a microwave pulse that covers the 6.95–18.45 GHz frequency range following frequency up-conversion with the PDRO.

The two strategies to reduce sample consumption described in Ref. [14] were implemented. Sample introduction into the vacuum chamber used two pulsed valve sources operated with 700 μs pulse duration. The nozzles inject the sample perpendicular to the microwave propagation. For each sample injection cycle, 10 separate broadband rotational spectra were acquired. The individual broadband chirped pulses were separated by 25 μs. The rotational free induction decay was acquired for 20 μs following each 1 μs excitation pulse. The repetition rate for the sample injection was 0.6 Hz and is limited by the data processing rate of the digital oscilloscope. A total of 288 000 rotational spectra of 1,2-propanediol were acquired in 28 800 injection cycles with a total measurement duration of approximately 14 h. The sample conditions for the broadband FTMW measurements were the same as the cavity FTMW measurements described above.

3. Ab initio calculations

Previously Vázquez et al. [4] reported optimized geometries for 23 conformers from ab initio calculations with a 4-21G basis set. We have re-examined 10 of the lowest energy forms whose calculated energies were below 12.6 kJ/mol (1056 cm^{-1}). The theoretical study of the ten conformers of 1,2-propanediol was initially performed at the MP2/6-311G(d) [16] level using the GAUSSIAN 03 Quantum Chemistry Package [15,17]. Each of the geometric isomers was fully optimized at the MP2/aug-cc-pVTZ level and shown in Figs. 1 and 2. All geometries were at true energy minima as verified in calculations of the analytical second derivatives. The relative energies of the 10 conformers with and without zero-point-energy (ZPE) corrections are summarized in Table 1. The predicted rotational constants and dipole moment components are also reported in the Table 1 and used below to aid the identification of the experimentally observed forms. The structural parameters of the six lowest energy forms observed are given in Tables 2 and 3 according to the labeling given in Fig. 1. Structural parameters of the remaining four conformers may be found in the supplementary material. The conformer labels used in Table 1 and subsequent tables use those from Vázquez et al. [4] for conformers 1 to 9. Conformer 10 here is conformer 12 in Ref. [4].

Rather interestingly, in Ref. [4] conformer 1 was found to be the lowest energy conformation, while in the higher level calculations presented here, conformer 3 is the lowest in energy. On the other hand in the laboratory study by Caminati [8], where only conformers 1 and 2 were assigned, it was concluded that conformer 2 was the lower energy form.

4. Results and analysis

The analysis was started using rotational constants reported in the previous study by Caminati [8]. Predictions based on these data allowed us to readily assign new spectral lines for the two conformers identified by Caminati. For conformer 1 (g′Gt), 32 new transitions were assigned and for conformer 2 (gG′t), 41 new transitions were assigned over the frequency range of 6.4–25 GHz. These transitions were fitted together with the data from Ref. [8] with a fit deviation of about 2 kHz for the currently measured data. The measurements, assignments and residuals of the fits for conformers 1 and 2 are shown in the supplementary tables. The improved values of rotational and centrifugal distortion constants are given in Table 4.

Once the two previously known conformers were completely assigned, we examined the remaining spectral lines for evidence of any of the other conformers based on the ab initio results in Table 1. Conformer 3 was easily assigned since its a-type transitions were the same intensity as those of conformer 2 and only offset in frequency by 10's of MHz and conformer 3 was calculated to be the lowest energy form. We also managed to assign a rather weak set of spectral lines found in the NIST FTMW scan to conformer 4, which has the highest calculated energy of conformers 1 to 4. The assigned spectral lines for conformer 3 are shown in Table 5 and those for conformer 4 are listed in Table 6 along with the residuals of the fits. Table 7 lists the fitted molecular constants for both conformers 3 and 4 and compares them with the theoretical rotational constants.

In order to determine if any other higher energy conformers might be assigned as well as ^{13}C isotopologues of the low energy forms, deep integration scans were carried out using the University of Virginia spectrometer. In addition, since this instrument has no cavity or waveguide to make relative intensity measurements difficult, this spectrum can give the best experimental determination of the relative energies of the various conformers when coupled to the theoretical or experimental dipole moments (described in Section 5). From the new deep integration data shown in Fig. 3, three more spectra were assigned. Two were easily identified as belonging to the conformers 5 and 6 based on agreement with the rotational constants as listed in Table 8. The remaining conformer has rotational constants very similar to those calculated for conformers 4, 7 and 8. The rotational analysis of this last (7th conformer) is shown in Table 9 along with a comparison to the theoretical values calculated for conformers 7 and 8. In order to provide a more definitive assignment of these two spectra for conformers "4" and "7", the calculated dipole moment components squared were used to simulate the relative intensities and compared to the observed spectra. For conformer 4 observed we find relative intensities of 69%, 14% and 17% for the a-type, b-type and c-type transitions, respectively, by normalizing the relative intensities to 100%. Comparing these to the ratio of the calculated dipole moment squared and total dipole moment squared, which are 72%, 24% and 15%, we find good agreement with the a- and c-type and a bit poorer agreement with the b-type. For conformer 7 observed we find relative intensities of 24%, 10% and 66% for the a-type, b-type and c-type transitions, respectively, by normalizing

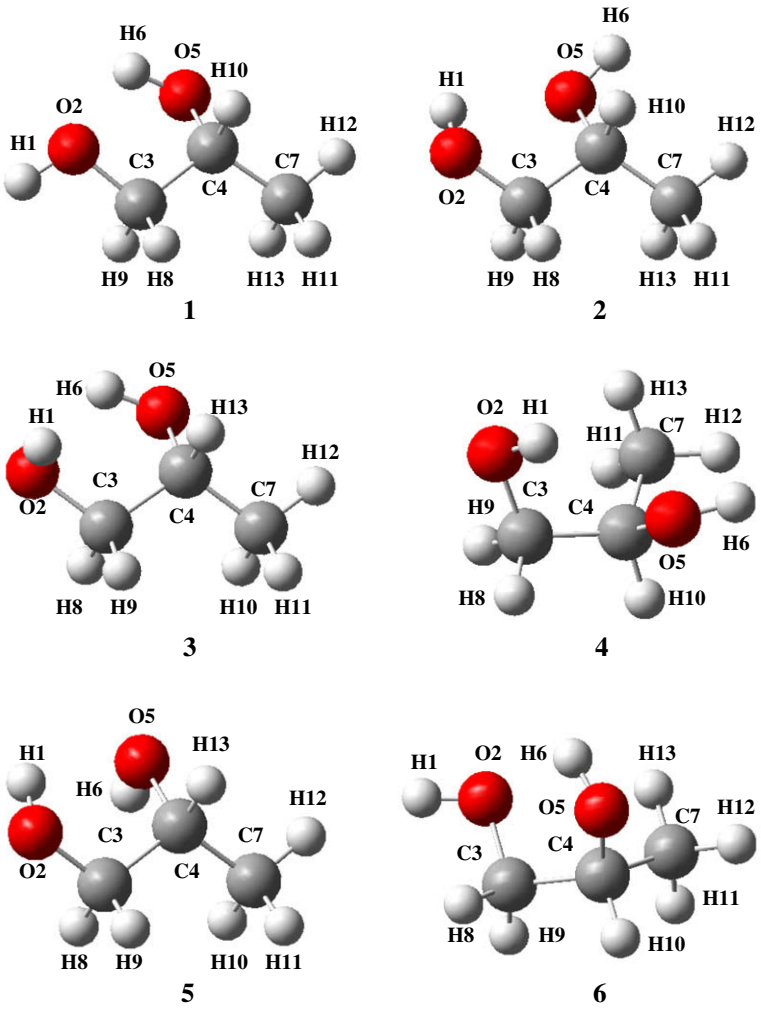

Fig. 1. The conformers 1 to 6 of 1,2-propanediol determined from ab initio MP2/aug-cc-pVTZ calculations. Atom labels correlate with structural parameters given in Tables 2 and 3 and in the supplement tables.

the relative intensities to 100%, compared to the ratio of the calculated dipole moment squared and total dipole moment squared for conformer 7 of 18%, 12% and 70%, which is very good agreement with the all three components. Noting that the observed conformer 4 is dominated by the a-type transitions and conformer 7 by c-type transitions, then these two assignments seem quite reasonable, since for calculated conformer 4, μ_a is the largest component (-6.41×10^{-30} C m or -1.92 D) and for conformer 7, μ_c is largest (6.37×10^{-30} C m or 1.91 D), while for conformer 8, μ_b dominates (8.31×10^{-30} C m or 2.49 D).

Once we had completed the measurements and assignments reported above, we learned of a recent FTMW study of 1,2-propanediol by Lockley et al. [18] in which conformer 3 was identified and found to be the lowest in energy of 27 conformers whose geometry was calculated with the HF/6-31G level of theory. There is excellent agreement between our results and those of Lockley et al. [18] where comparison can be made with experimental and theoretical values.

The observed and calculated rotational constants for the $^{13}C_n$ species of a number of the conformers with the more intense spectra are given in Table 10. The calculated values were obtained from the ab initio structures where the difference between the theoretical values for the normal species and the ^{13}C species was applied to the observed rotational constants. Agreement was found to be within several MHz which further strengthens the validity of the assignments. Lockley et al. [18] also measured the ^{13}C isotopologes of conformer 3 and there is excellent agreement between their rotational constants and ours, although they had an insufficient number of transitions to fit the centrifugal distortion constants.

5. Dipole moment determination

One of the NIST FTMW spectrometers is equipped with a set of 25 cm × 25 cm parallel plates separated by 25 cm [19]. These are positioned along the cavity axis centered between the mirrors and the nozzle located perpendicular to the cavity axis. Positive voltage is applied to one plate and an equal negative voltage is applied to the second plate to obtain Stark effect shifts in the transitions. The microwave electric field and external electric field are parallel so that $\Delta M = 0$ transitions are observed. The precise Stark plate separation, d, was determined by a calibration with OCS $J = 1$–0 transition and the known dipole moment of $\mu = 2.3856(10) \times 10^{-30}$ C m (0.71519(3) D) [20,21].

For conformer 1, the $M = 0$ and 1 components of the 2(0, 2)–1(0, 1), and 2(1, 1)–1(1, 0) a-type and 2(1, 1)–1(0, 1) c-type transitions were measured with applied voltages up to 5 kV (plus and minus 2.5 kV) with frequency shifts up to 1 MHz. For conformer 2, the $M = 0$ and 1 components of the 2(1, 2)–1(1, 1), 2(0, 2)–1(0, 1) and 2(1, 1)–1(1, 0) a-type and the $M = 0$ component of the 1(1, 0)–0(0, 0), c-type transition were measured with voltages up to 4.5 kV (plus and minus 2.25 kV) and maximum shift up to

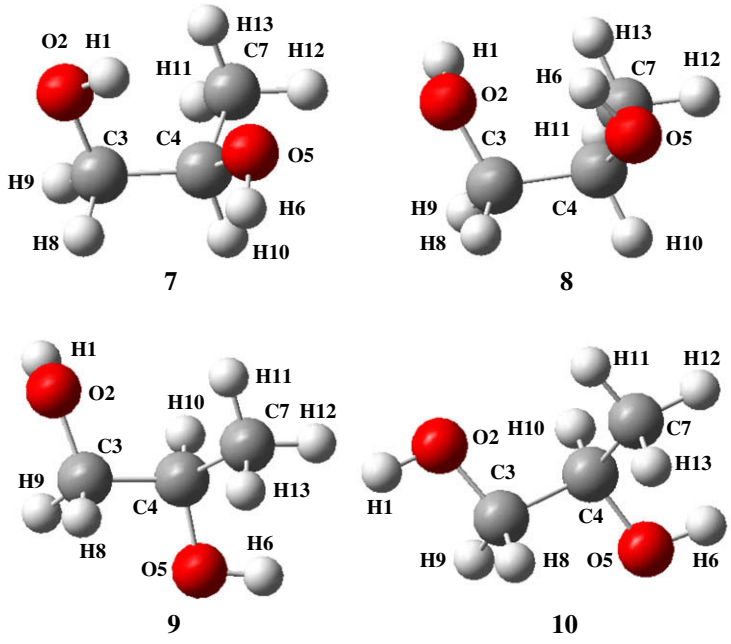

Fig. 2. The conformers 7 to 10 of 1,2-propanediol determined from ab initio MP2/aug-cc-pVTZ calculations. Atom labels correlate with structural parameters given in the supplement tables.

Table 1
Theoretical rotational constants, dipole moments and energies for the 1,2-propanediol conformers from MP2/aug-cc-pVTZ.

#[a]	ID[a]	*A* (MHz)	*B* (MHz)	*C* (MHz)	μ_a (10^{-30} C m)	μ_b (10^{-30} C m)	μ_c (10^{-30} C m)	ΔE (cm^{-1})	ΔE (cm^{-1})[b]	ΔE (kJ mol^{-1})[b]
1	g′Gt	6672.3	4213.2	3407.2	7.84 (2.35 D)[c]	−1.00 (−0.30 D)[c]	2.34 (0.70 D)[c]	192	212	2.54
2	gG′t	8451.8	3678.9	2802.6	−8.81 (−2.64 D)	0.93 (0.28 D)	−1.90 (−0.57 D)	83	74	0.89
3	tG′g	8643.1	3672.6	2818.1	4.04 (1.21 D)	−7.00 (−2.10 D)	1.50 (0.45 D)	0	0	0.0
4	tGg′	6654.0	4217.7	3424.7	−6.41 (−1.92 D)	−3.97 (−1.19 D)	3.14 (0.94 D)	338	349	4.17
5	g′G′g	8608.5	3630.1	2802.3	−1.37 (−0.41 D)	−6.20 (−1.86 D)	−5.04 (−1.51 D)	87	115	1.37
6	gG′g′	8371.4	3574.6	2801.0	−7.54 (−2.26 D)	−2.34 (−0.70 D)	3.97 (1.19 D)	213	230	2.75
7	g′Gg	6659.2	4192.8	3407.8	3.27 (0.98 D)	2.67 (0.80 D)	6.37 (1.91 D)	345	375	4.49
8	gGg′	6647.6	4160.1	3369.6	−1.17 (−0.35 D)	−8.31 (−2.49 D)	1.17 (0.35 D)	441	481	5.75
9	tT′t′	8044.7	3702.3	2776.7	−0.27 (−0.08 D)	0.77 (0.23 D)	0.47 (0.14 D)	862	752	9.00
10	gT′t′	7982.0	3632.7	2751.6	3.07 (0.92 D)	2.00 (0.60 D)	−5.34 (−1.60 D)	929	838	10.0

[a] Notation employed by Vázquez et al. [4].
[b] Zero point energies (ZPE) included. Conversion factor 1 kJ mol^{-1} = 83.594 cm^{-1}.
[c] In Debye. 1 D = 3.336 × 10^{-30} C m.

Table 2
Structural bond distance from the MP2 calculations for the observed conformers 1 to 6 (Å) of 1,2-propanediol.

Distance	Conf. 1 g′Gt′	Conf. 2 gG′t	Conf. 3 tG′g	Conf. 4 t′Gg′	Conf. 5 g′G′g	Conf. 6 gG′g′
O2–H1	0.9656	0.9655	0.9617	0.9616	0.9633	0.9665
C3–O2	1.4185	1.4170	1.4300	1.4309	1.4299	1.4159
C4–C3	1.5174	1.5133	1.5126	1.5168	1.5163	1.5172
O5–C4	1.4345	1.4351	1.4232	1.4245	1.4219	1.4354
H6–O5	0.9629	0.9628	0.9664	0.9664	0.9671	0.9653
C7–C4	1.5158	1.5156	1.5115	1.5198	1.5118	1.5143
H8–C3	1.0939	1.0891	1.0936	1.0918	1.0932	1.0900
H9–C3	1.0892	1.0959	1.0935	1.0936	1.0896	1.0986
H10–C4	1.0958	1.0945	1.0964	1.0913	1.0993	1.0905
H11–C7	1.0901	1.0904	1.0897	1.0907	1.0899	1.0899
H12–C7	1.0912	1.0900	1.0880	1.0880	1.0881	1.0882
H13–C7	1.0880	1.0895	1.0897	1.0891	1.0896	1.0923

1.4 MHz. For conformer 3, the $M = 0$ component of the b-type 1(1, 1)–0(0, 0) transition and $M = 0$ and 1 components of the 2(0, 2)–1(0, 1), and 2(1, 2)–1(1, 1) a-type and 2(1, 1)–1(0, 1) c-type transitions were measured with applied voltages up to 6 kV (plus and minus 3 kV) with frequency shifts up to 1.2 MHz. The Stark shifts were least-squares fit to the standard second-order asymmetric rotor coefficients of $(\mu_x E)^2$, where x = a, b, c, to derive the μ_a, μ_b and μ_c dipole moment components listed in Table 11 with comparisons to the ab initio values.

6. Astronomical observations

Observations of 1,2-propanediol, conformers 2 and 3 were made as part of the Green Bank Telescope (GBT) Prebiotic

Table 3
Structural bond angles from the MP2 calculations for conformers 1 to 6 (degree).

Angle	Conf. 1 g′Gt′	Conf. 2 gG′t	Conf. 3 tG′g	Conf. 4 t′Gg′	Conf. 5 g′G′g	Conf. 6 gG′g′
C3–O2–H1	105.1°	105.7°	105.1°	105.1°	108.1°	105.6°
C4–C3–O2	111.8°	111.8°	111.8°	111.8°	111.0°	111.4°
O5–C4–C3	104.6°	104.6°	104.6°	104.6°	109.6°	108.9°
H6–O5–C4	108.3°	108.5°	108.3°	108.3°	106.1°	107.5°
C7–C4–C3	112.8°	111.9°	112.8°	112.8°	111.8°	112.2°
C7–C4–O5	111.5°	111.6°	111.5°	111.5°	107.8°	111.8°
H8–C3–O2	110.8°	106.9°	110.8°	110.8°	111.3°	107.1°
H8–C3–C4	108.8°	109.9°	108.8°	108.8°	110.6°	110.3°
H9–C3–O2	106.9°	111.1°	106.9°	106.9°	105.6°	110.9°
H9–C3–C4	109.9°	108.5°	109.9°	109.9°	109.2°	108.8°
H9–C3–H8	108.6°	108.7°	108.6°	108.6°	108.9°	108.1°
H10–C4–C3	108.1°	108.4°	108.1°	108.1°	108.4°	108.6°
H10–C4–O5	109.6°	109.4°	109.6°	109.6°	109.5°	104.2°
H10–C4–C7	110.1°	110.7°	110.1°	110.1°	109.6°	110.6°
H11–C7–C4	110.3°	110.6°	110.3°	110.3°	110.8°	110.7°
H12–C7–C4	110.7°	110.8°	110.7°	110.7°	110.0°	110.4°
H12–C7–H11	107.8°	108.0°	107.8°	107.8°	108.7°	108.6°
H13–C7–C4	110.2°	110.0°	110.2°	110.2°	109.9°	110.5°
H13–C7–H11	108.8°	109.0°	108.8°	108.8°	109.1°	108.0°
H13–C7–H12	109.1°	108.3°	109.1°	109.1°	108.4°	108.6°
C4–C3–O2–H1	−52.7° g′	49.9° g	167.0° t	−164.1° t′	−75.1° g′	42.6° g
H8–C3–O2–H1	68.8°	170.2°	−73.2°	−45.6°	48.6°	163.3°
H9–C3–O2–H1	−173.0°	−71.4°	48.7°	75.9°	166.7°	−78.9°
O5–C4–C3–O2	60.7° G	−59.6° G′	−58.9° G′	60.9° G	−54.8° G′	−54.7° G′
C7–C4–C3–O2	−60.6°	179.4°	−178.2°	−63.3°	−174.3°	−179.0°
O5–C4–C3–H8	−67.0°	−178.2°	−179.2°	−58.5°	61.3°	−173.5°
C7–C4–C3–H8	176.7°	60.9°	61.5°	177.2°	61.6°	62.1°
O5–C4–C3–H9	179.2°	63.2°	60.7°	−178.7°	61.3°	68.0°
C7–C4–C3–H9	57.9°	−57.7°	−58.6°	57.1°	−58.2°	−56.4°
H10–C4–C3–O2	177.4°	57.1°	60.6°	175.5°	64.8°	58.3°
H10–C4–C3–H8	54.7°	−61.5°	−59.7°	56.0°	−59.3°	−60.5°
H10–C4–C3–H9	−64.1°	179.9°	−179.8°	−64.1°	−179.2°	−179.0°
H6–O5–C4–C3	−167.3° t′	169.3° t	48.2° g	−50.7° g′	41.6° g	−77.0° g′
H6–O5–C4–C7	−45.1°	−69.5°	169.9°	70.4°	163.5°	47.7°
H6–O5–C4–H10	77.0°	53.4°	−70.4°	−166.8°	−77.3°	167.2°
H11–C7–C4–C3	−64.2°	−62.2°	−61.4°	−61.2°	−62.1°	−60.4°
H11–C7–C4–O5	178.5°	−179.0°	178.0°	175.5°	177.3°	176.9°
H11–C7–C4–H10	56.7°	58.9°	58.5°	58.9°	58.2°	61.1°
H12–C7–C4–C3	176.6°	178.1°	178.5°	178.7°	177.8°	179.2°
H12–C7–C4–O5	59.3°	61.3°	57.9°	55.4°	57.2°	56.5°
H12–C7–C4–H10	−62.5°	−60.8°	−61.5°	−61.2°	−61.9°	−59.2°
H13–C7–C4–C3	55.9°	58.3°	59.3°	58.9°	58.5°	59.2°
H13–C7–C4–O5	−61.4°	−58.5°	−61.3°	−64.5°	−62.0°	−63.6°
H13–C7–C4–H10	176.8°	179.4°	179.3°	179.0°	178.8°	−179.3°

Table 4
Rotational constants for conformers 1 and 2 of 1,2-propanediol from the A-reduction Hamiltonian.

Parameter	Conf. 1 g′Gt	Theory[b]	Diff. (%)	Conf. 2 gG′t	Theory[b]	Diff. (%)
A (MHz)	6642.4488(9)[a]	6672.3	−0.5	8393.4003(16)[a]	8451.8	−0.7
B (MHz)	4163.5949(9)	4213.2	−1.2	3648.5661(7)	3678.9	−0.8
C (MHz)	3365.3627(7)	3407.2	−1.2	2778.2963(6)	2802.6	−0.9
Δ_J (kHz)	1.774(29)	1.80	−1.4	0.797(15)	0.772	3.1
Δ_{JK} (kHz)	6.354(82)	5.55	13	4.485(70)	4.88	−8.7
Δ_K (kHz)	−4.51(12)	−3.28	27	3.16(35)	3.44	−5.8
d_J (kHz)	0.267(13)	0.254	4.9	0.1827(60)	0.177	3.1
d_K (kHz)	1.74(18)	0.89	49	3.14(21)	2.96	5.7
N_{lines}	46			61		
Wt. Std.[c]	0.63			0.90		
Energy (kJ mol^{-1})		2.54			0.89	

[a] Uncertainties shown in parentheses refer to the last digits shown and are Type A, coverage factor $k = 2$ (two standard deviations) [21].
[b] Anharmonic contributions to the centrifugal distortion terms were not calculated.
[c] Weighted standard deviation, unitless, with weights of the reciprocal of the uncertainties squared.

Interstellar Molecule Survey (PRIMOS) Legacy Project [22] between January and May 2008 with the NRAO[1] 100 m Robert C. Byrd Green Bank Telescope (GBT). The GBT spectrometer was configured in its eight intermediate-frequency (IF), 200 or 800 MHz, three-level mode, which provides for observing four 200 MHz frequency bands or four 800 MHz frequency bands at a time in two polarizations through the use of offset oscillators in the IF part of the receiver. Antenna temperatures are on the T_A^* scale [23] with estimated standard uncertainties of 20%. The Sgr B2 (N-LMH) J2000 pointing position

[1] The National Radio Astronomy Observatory is a facility of the National Science Foundation, operated under cooperative agreement by Associated Universities, Inc.

Table 5
Microwave spectrum of conformer 3 (tG′g) of 1,2-propandiol found to be the lowest energy conformer.

J'	K_a'	K_c'	–	J''	K_a''	K_c''	Conformer 3-tG′g Frequency (Unc.) (MHz)	Obs.–Calc. (kHz)
1	0	1	–	0	0	0	6431.070(5)	0
2	1	1	–	2	0	2	6730.650(5)	1
2	0	2	–	1	1	0	6980.572(5)	−2
5	1	5	–	4	2	2	7764.398(5)	−1
2	0	2	–	1	1	1	7829.698(5)	−1
5	2	3	–	4	3	2	7940.322(5)	−6
6	2	5	–	6	1	5	8231.030(5)	1
3	1	2	–	3	0	3	8330.237(2)	1
4	1	3	–	4	1	4	8439.098(5)	0
7	2	5	–	7	2	6	9135.908(5)	1
5	1	5	–	4	2	3	9187.456(5)	−1
5	2	4	–	5	1	4	10212.644(5)	4
6	2	5	–	5	3	2	10336.392(5)	−1
4	1	3	–	4	0	4	10733.597(2)	0
1	1	1	–	0	0	0	11363.016(2)	3
2	1	2	–	1	1	1	12012.979(2)	0
4	2	3	–	4	1	4	12037.136(2)	2
3	0	3	–	2	1	1	12169.580(5)	1
1	1	0	–	0	0	0	12212.139(2)	1
5	1	4	–	5	1	5	12531.724(5)	−1
2	0	2	–	1	0	1	12761.642(2)	0
4	1	3	–	3	2	1	13115.007(2)	1
5	2	3	–	5	1	4	13321.315(2)	0
4	2	2	–	4	1	3	13460.192(2)	1
3	2	2	–	3	1	2	13588.939(2)	3
4	1	3	–	3	2	2	13608.395(2)	−2
2	1	1	–	1	1	0	13711.223(2)	0
6	2	4	–	6	1	5	13904.984(2)	0
5	1	4	–	5	0	5	14024.219(2)	2
3	2	1	–	2	1	2	14082.330(2)	3
3	0	3	–	2	1	2	14716.948(2)	1
2	2	1	–	2	1	1	14795.734(2)	−1
2	2	0	–	2	1	1	14896.214(2)	−1
7	2	6	–	6	3	3	15243.724(5)	3
7	2	5	–	7	1	6	15388.141(2)	−2
4	0	4	–	3	1	2	16463.736(2)	−1
2	1	2	–	1	0	1	16944.923(2)	1
6	1	5	–	6	1	6	17233.586(5)	4
2	2	1	–	2	1	2	17343.103(4)	−5
2	2	0	–	2	1	2	17443.584(4)	−4
8	2	6	–	8	1	7	17887.912(5)	8
3	1	3	–	2	1	2	17959.964(2)	0
3	0	3	–	2	0	2	18900.228(2)	1
3	1	2	–	2	1	1	20499.815(2)	0
4	0	4	–	3	1	3	21550.957(2)	0
5	1	4	–	4	2	3	21719.183(2)	1
3	1	3	–	2	0	2	22143.244(2)	0
5	2	4	–	5	1	5	22744.365(2)	0
7	1	6	–	7	0	7	22870.650(2)	−1
6	3	3	–	6	2	4	23335.474(2)	−1
4	1	4	–	3	1	3	23845.456(2)	0
5	3	2	–	5	2	2	24692.828(2)	2
4	0	4	–	3	0	3	24793.974(2)	1
4	2	3	–	3	2	2	25645.529(2)	−2
4	3	2	–	3	3	1	25904.113(4)	−2
4	3	1	–	3	3	0	25948.658(4)	−3

[a]Uncertainties refer to the last digit and are Type B coverage factor $k = 2$ [21].

employed in azimuth and declination was $\alpha = 17^h47^m19.^s8$ and $\delta = -8°22'17''$, and a local standard of rest source velocity of +64 km s^{-1} was assumed. Data were taken in the OFF–ON position-switching mode, with the OFF position 60′ east in azimuth with respect to the ON-source position. A single scan consisted of 2 min in the OFF-source position followed by 2 min in the ON-source position. Automatically updated dynamic pointing and focusing corrections were employed based on real-time temperature measurements of the structure input to a thermal model of the GBT; zero points were adjusted typically every 2 h or less using the quasar 1733-130 for calibration. The two polarization outputs from the spectrometer were averaged in the final data reduction process to improve the signal-to-noise ratio.

For conformer 3 five b-type transitions (μ_b = 1.9 D, see Table 11) were searched for including the 2(0, 2)–1(1, 1) at 7829.700 MHz, the 3(0, 3)–2(1, 2) at 14716.948 MHz, the 4(0, 4)–3(1, 3) at 21550.957 MHz, the 5(0, 5)–4(1, 4) at 28171.196 MHz and the 6(0, 6)–5(1, 5) at 34511.637 MHz. The full spectroscopic parameters of each transition including the calculated and measured rest frequencies, transition line strengths, and lower level energies can be found in Table 12. No transitions were detected beyond the 1-sigma rms noise limit in any of the observed passbands. The lowest noise level attained was ≈4 mK at 14716.948 MHz. Using the formalism presented by Hollis et al. [24] to calculate total column density and assuming a temperature of 10 K, which is consistent with other large organic species detected with the GBT toward

Table 6
Microwave spectrum of conformer 4 (tGg′) of 1,2-propandiol.

J'	K_a'	K_c'	–	J''	K_a''	K_c''	Conformer 4-tGg′ Frequency (Unc.) (MHz)	Obs.–Calc. (kHz)
4	2	2	–	4	1	3	7104.172(5)	−1
1	0	1	–	0	0	0	7538.530(5)	−4
2	2	0	–	2	1	1	7580.520(5)	−1
4	1	3	–	4	0	4	8337.544(5)	−1
2	2	1	–	2	1	2	9770.492(5)	0
2	2	0	–	2	1	2	9928.654(5)	−1
1	1	1	–	0	0	0	10012.656(5)	−2
1	1	0	–	0	0	0	10795.372(5)	−2
3	2	2	–	3	1	3	11034.964(5)	−2
2	0	2	–	1	1	0	11662.018(5)	−5
3	2	1	–	3	1	3	11787.314(5)	3
2	0	2	–	1	1	1	12444.740(2)	1
4	2	3	–	4	1	4	12740.140(5)	−1
4	3	1	–	4	2	2	12894.760(5)	0
3	3	0	–	3	2	1	13686.086(5)	0
2	1	2	–	1	1	1	14294.285(2)	2
3	3	1	–	3	2	2	14417.958(5)	−2
3	3	0	–	3	2	2	14438.430(5)	−2
2	0	2	–	1	0	1	14918.861(2)	−2
2	1	1	–	1	1	0	15859.702(2)	−1
3	1	2	–	2	2	0	16097.870(5)	−1
2	1	2	–	1	0	1	16768.407(2)	0
2	1	1	–	1	0	1	19116.541(2)	−1
3	0	3	–	2	1	2	20171.707(2)	1
3	1	3	–	2	1	2	21350.763(2)	0
3	0	3	–	2	0	2	22021.252(2)	1
3	2	2	–	2	2	1	22615.237(2)	0
3	1	3	–	2	0	2	23100.306(2)	−2
3	2	1	–	2	2	0	23209.420(2)	1
2	2	1	–	1	1	0	23282.062(2)	2
2	2	0	–	1	1	0	23440.224(2)	1
3	1	2	–	2	1	1	23678.391(2)	0

[a]Uncertainties refer to the last digit and are Type B coverage factor $k = 2$ [21].

Table 7
Rotational constants for conformers 3 and 4 of 1,2-propanediol from the A-reduction Hamiltonian.

Parameter	Conformer 3 tG′g	Theory[b]	Diff. (%)	Conformer 4 tGg′	Theory[b]	Diff. (%)
A (MHz)	8572.0553(8)[a]	8643.1	−0.8	6634.7621(7)[a]	6654.0	−0.3
B (MHz)	3640.1063(5)	3672.6	−0.9	4160.6347(9)	4217.7	−1.4
C (MHz)	2790.9666(4)	2818.1	−1.0	3377.9063(8)	3424.7	−1.4
Δ_J (kHz)	0.738(7)	0.719	2.6	1.751(31)	1.74	0.6
Δ_{JK} (kHz)	5.276(30)	5.56	−5.4	8.21(11)	7.47	9.0
Δ_K (kHz)	2.53(10)	2.97	−17	−6.51(12)	−4.86	25
d_J (kHz)	0.1631(16)	0.155	4.9	0.244(17)	0.244	0
d_K (kHz)	3.180(31)	3.16	0.6	2.72(23)	1.61	40
N_{lines}	57			32		
Wt. Std.[c]	0.88			0.57		
Energy (kJ mol^{-1})		0.0			4.17	

[a] Uncertainties shown in parentheses refer to the last digits shown and are Type A, coverage factor $k = 2$ (two standard deviations) [21].
[b] Anharmonic contributions to the centrifugal distortion terms were not calculated.
[c] Weighted standard deviation, unitless, with weights of the reciprocal of the uncertainties squared.

the SgrB2N extended envelope [24], we find an upper limit to the 1,2-propanediol conformer 3 total column density of $N_T < 8 \times 10^{14}$ cm^{-2}. This is assuming a rotational partition function of 18.1 $T^{1.5}$ found from the measured A, B and C rotational constants.

Before we determined that conformer 3 was the lowest energy form, we searched for conformer 2 (83 cm^{-1} in energy above conformer 3) using the GBT PRIMOS legacy Project data [17]. Six a-type transitions ($\mu_a = 2.5$ D, see Table 11) were searched for, including the 2(0, 2)–1(0, 1) at 12744.622 MHz, the 3(0, 3)–2(0, 2) at 18855.110 MHz, the 5(0, 5)–4(0, 4) at 30331.389 MHz, the 6(0, 6)–5(0, 5) at 35831.471 MHz, the 7(0, 7)–6(0, 6) at 41300.113 MHz and the 8(0, 8)– 7(0, 7) at 46783.202 MHz. The full set of spectroscopic parameters of each transition can once again be found in Table 12. No transitions were detected beyond the 1-sigma rms noise limit in any of the observed passbands. The lowest noise level attained was ≈2 mK at 18855.109 MHz. Again using the formalism presented by Hollis et al. [24] to calculate total column density and assuming a temperature of 10 K, we find an upper limit to the total 1,2-propanediol conformer 2 column density of $N_T < 2 \times 10^{14}$ cm^{-2}. This is assuming a rotational partition function of 18.3 $T^{1.5}$ derived from the measured A, B and C rotational constants and ignoring the energy offset between the conformers.

The measured abundance of glycolaldehyde ($CHOCH_2OH$) is $N_T \approx 3 \times 10^{14}$ cm^{-2} toward Sgr B2N [24]. The abundance for ethylene glycol can be derived from the 2_{02} ($v = 0$) to 1_{01} ($v = 1$) transition at 13380.6 MHz reported by Hollis [25]. Assuming a temperature of 10 K, the total average column density of ethylene glycol for the entire line complex, consisting of 82, 73 and 64 km/s components with a peak intensity of $T_A = 20$ mK, is 3.3×10^{14} cm^{-2}

Table 8
Rotational constants for conformers 5 and 6 of 1,2-propanediol from the A-reduction Hamiltonian.

Parameter	Conformer 5 tG′g	Theory[b]	Diff. (%)	Conformer 6 tGg′	Theory[b]	Diff. (%)
A (MHz)	8536.77 0(2)[a]	8608.5	−0.8	8327.599(5)[a]	8371.4	−0.5
B (MHz)	3604.198(1)	3630.1	−0.9	3642.001(4)	3674.6	−0.9
C (MHz)	2778.331(1)	2802.3	−1.0	2776.902(3)	2801.0	−0.9
Δ_J (kHz)	0.751(14)	0.714	4.9	0.76(12)	0.767	−1.3
Δ_{JK} (kHz)	5.29(7)	5.66	−8.1	5.1(6)	4.81	5.9
Δ_K (kHz)	2.75(22)	2.99	−8.7	2.9 (fixed)	2.89	–
d_J (kHz)	0.152(6)	0.143	5.9	0.24(11)	0.166	29
d_K (kHz)	3.34(14)	3.12	6.6	2.8(fixed)	2.85	–
N_{lines}	44			18		
Wt. Std.[c]	1.1			1.9		
Energy (kJ mol^{-1})		0.88			2.75	

[a] Uncertainties shown in parentheses refer to the last digits shown and are Type A, coverage factor $k = 2$ (two standard deviations) [21].
[b] Anharmonic contributions to the centrifugal distortion terms were not calculated.
[c] Weighted standard deviation, unitless, with weights of the reciprocal of the uncertainties squared.

Table 9
Rotational constants for conformers 7 and 8 of 1,2-propanediol from the A-reduction Hamiltonian.

Parameter	Conformer 7 Obs.	Conformer 7 Theory tG′g	Diff. (%)	Conformer 8 Theory tGg′	Diff. (%)
A (MHz)	6627.612(8)	6659.2	−0.5	6647.6	−0.3
B (MHz)	4146.287(5)	4192.7	−1.1	4169.1	−0.5
C (MHz)	3363.345(6)	3407.8	−1.3	3369.6	−0.2
Δ_J (kHz)	1.84(3)	1.83	0.5	1.74	5.4
Δ_{JK} (kHz)	6.2(2)	5.85	4.8	7.61	23
Δ_K (kHz)	−5.0(3)	−3.84	23	−5.05	−2
d_J (kHz)	0.23(3)	0.249	8.7	0.247	8.7
d_K (kHz)	1.8(3)	1.19	33	2.06	−16
N_{lines}	20				
Wt. Std.[b]	0.5				
Energy (kJ mol^{-1})		4.49		5.75	

[a] Uncertainties shown in parentheses refer to the last digits shown and are Type A, coverage factor $k = 2$ (two standard deviations) [21].
[b] Weighted standard deviation, unitless, with weights of the reciprocal of the uncertainties squared.
[c] Value fixed at the average values from conformers 1 and 4.

Table 10
Observed and calculated rotational constants for the ^{13}C isotopologues.

Conf./atom	A Obs. (MHz)	B Obs. (MHz)	C Obs. (MHz)	A Calc. (MHz)	B Calc. (MHz)	C Calc. (MHz)
1/$^{13}C_3$	6599.712(17)	4119.586(6)	3347.067(6)	6599.00	4118.57	3346.65
1/$^{13}C_4$	6622.622(27)	4143.717(10)	3357.691(9)	6621.71	4142.95	3357.24
1/$^{13}C_7$	6523.148(6)	4113.966(4)	3305.769(4)	6523.01	4112.88	3304.78
2/$^{13}C_3$	8314.741(6)	3633.983(4)	2763.027(4)	8313.19	3633.80	2762.76
2/$^{13}C_4$	8377.518(6)	3639.268(4)	2774.789(4)	8376.48	3638.84	2774.50
2/$^{13}C_4$	8327.826(6)	3565.701(4)	2723.004(4)	8328.32	3564.35	2722.24
3/$^{13}C_3$	8485.725(4)	3625.759(4)	2775.135(4)	8483.43	3625.55	2774.77
3/$^{13}C_4$	8555.920(4)	3631.166(2)	2787.564(2)	8554.84	3630.77	2787.29
3/$^{13}C_7$	8506.815(4)	3557.975(2)	2735.709(2)	8507.30	3556.70	2734.94
4/$^{13}C_3$				6588.71	4114.72	3359.36
4/$^{13}C_4$				6615.43	4140.52	3369.72
4/$^{13}C_7$				6513.61	4111.61	3317.03

and about equal to the glycolaldehyde abundance. The results for 1,2-propanediol are consistent with the assumption that as molecular complexity increases, i.e. adding a CH_2 group, the total column density of the molecule decreases. If the total column density of 1,2-propanediol is closer to $N_T = 3 \times 10^{13}$ cm^{-2}, then an rms noise level <0.2 mK will be needed to detect this species beyond the 1σ level which would require a further advance in sensitivity beyond the capabilities of the current instrumentation.

7. Discussion

During the course of this study, we employed three different FTMW spectrometers, two cavity types [10,11] and one broadband spectrometer [14]. Due to the various configurations, we also employed three different nozzle reservoir designs. In this process, we found that the heated nozzle design for the mini-FTMW spectrometer [26], which has an extension to keep sample deposits from forming in the mirror hole through which the molecular beam is introduced to the vacuum chamber, has a significantly warmer rotational temperature compared to similar heated reservoir nozzles without the extension, e.g. like that used in the Stark effect measurements. Since we were interested in observing higher energy conformers, the nozzle with the extension was used in the deep integration on the broadband spectrometer. For the Stark effect measurements the pulsed-beam was artificially warmed by using N_2 as a backing gas instead of Ne in order to observe conformer 1, which has an energy of about 192 cm^{-1}.

Table 11
Measured and calculated (MP2/aug-cc-pVTZ) dipole moments for 1,2-propanediol conformers 1-3.

Dipole component	Expt.[a]	MP2
Conf.1g′Gt		
μ_a (D)	2.202(4)	2.35
μ_b (D)	0. fixed	−0.03
μ_c (D)	0.616(10)	0.70
Conf.2 gG′t		
μ_a (D)	2.496(2)	−2.64
μ_b (D)	0.309(20)	0.28
μ_c (D)	0.45(8)	−0.57
Conf.3 tG′g		
μ_a (D)	1.201(3)	1.21
μ_b (D)	1.916(6)	−2.10
μ_c (D)	0.365(36)	0.45

[a] Uncertainties shown in parentheses refer to the last digits shown and are Type A, coverage factor $k = 2$ (two standard deviations) [21].

By using the broadband spectrometer's deep integration ability, we were able to assign three additional conformers with high signal-to-noise for a total of seven conformers identified. The higher energy conformers are difficult to assign with the small number of beam-pulse averages typically employed in cavity FTMW surveys. Usually we use a 20 beam-pulse average at 4 Hz repetition rate with 0.5 MHz steps for a survey. This configuration requires 5 h to cover 1 GHz, so a 12 GHz survey would take more than 60 h to complete, roughly four times as long as the 288 000 pulse CP-FTMW experiment, but with only a 20 pulse average which is comparable to a 20 000 pulse average in the CP-FTMW experiment. The configuration employed in the broadband spectrometer had the molecular beam perpendicular to the direction of the microwave propagation so a Doppler broadened linewidth of about 400 kHz was obtained. In spite of this, measurement uncertainties were typically 5 kHz. In contrast, the cavity spectrometer has linewidths of 5–10 kHz and about 100 times higher signal intensity than the broadband spectrometer for a single molecular beam/microwave pulse. Thus, the cavity spectrometer is intrinsically higher resolution (in the configurations employed) and capable of resolving hyperfine or internal rotation splittings when present. Thus, the two spectrometers are complementary in capabilities.

The centrifugal distortion constants for conformers 1 to 7 are listed in Tables 4 and 7–9 in addition to the rotational constants. These are compared with the values derived from the ab initio structure calculations that excluded anharmonic contributions. Generally the theoretical values agree to better than 10% where the experimental uncertainties are small, while the rotational constants agree with the theoretical values at the 1% level. It is interesting to note that one of the problem assignments, namely conformer 7, where both the rotational constants and centrifugal distortion constant agree equally well with either the theoretically calculated parameters shown in Table 9, the assignment of this spectrum rests entirely on the relative intensity comparisons with the calculated dipole moment components.

Because the relative intensities of the CP-FTMW spectrometer are accurate over a large dynamic range [14], the relative populations of different conformers can be determined from this data. The ab initio dipole moments reported in Table 1 were used to scale the observed intensities to population, assuming a weak pulse limit and a rotational temperature of 1 K. For each dipole component of each conformer, a scale factor was found which matched the intensities of a simulated spectrum to the experimental spectrum across the entire bandwidth of the spectrometer. This scale factor was divided by the square of the dipole moment in that principal axis direction, which provided a relative population estimate. Directions with small dipole components (<0.5 D) were excluded from this analysis due to the possibility of large fractional errors in the ab initio calculations. Different dipole directions of the same conformer yielded similar population estimates, within 25%. These estimates were averaged together for each conformer and are presented in Table 13. These populations are compared to the thermal equilibrium population at 60 °C, using the ZPE-corrected ab initio relative energies, and an effective temperature is determined for each conformer relative to the most populated conformer.

These results confirm that conformer 3, as predicted by the ab initio calculations presented in Table 1, is in fact the most populated conformer in the supersonic expansion. Previously, Ruoff et al. [27] determined that conformational relaxation in inert carrier gases occurs when barriers to interconversion are less than 400 cm^{-1}. In the 1,2-propanediol system, the simplest and lowest energy interconversion pathway between different conformers is for the H atom bonded to the hydrogen-bond-accepting O atom to rotate by ≈110–120°. The eight lowest energy conformers are oriented in Fig. 4 to better illustrate these pathways. They are also first separated into two sets depending on the in-plane or out-of-plane orientation of the terminal oxygen atom relative to the carbon atoms. As illustrated by arrows, conformer 5 can relax by free OH rotation into conformer 3, conformer 7 into conformer 1, conformer 6 into conformer 2 and conformer 8 into conformer 4. In fact, the experimentally determined relative populations given in Table 13 indicate that three

Table 12
Transitions of 1,2-propanediol sought toward in Sgr B2(N-LMH).

J'	K_a'	K_c'	–	J''	K_a''	K_c''	Frequency (MHz)	E (K)	S_{ij}	T_A (mK)
Conformer 3										
2	0	2	–	1	1	1	7829.700	0.545	0.622	<8
3	0	3	–	2	1	2	14716.948	1.122	1.394	<4
4	0	4	–	3	1	3	21550.957	1.984	2.319	<8
5	0	5	–	4	1	4	28171.196	3.128	3.350	<8
6	0	6	–	5	1	5	34511.637	4.552	4.420	<8
Conformer 2										
2	0	2	–	1	0	1	12744.621	0.308	1.990	<5
3	0	3	–	2	0	2	18855.109	0.919	2.961	<2
5	0	5	–	4	0	4	30331.389	2.939	4.874	<8
6	0	6	–	5	0	5	35831.471	4.466	5.844	<5
7	0	7	–	6	0	6	41300.113	6.185	6.829	<8
8	0	8	–	7	0	7	46783.201	8.167	7.821	<8

[a]Uncertainties refer to the last digit and are Type B coverage factor $k = 2$ [21].

Table 13
Relative populations of conformers 1-7 of 1,2-propanediol.

Conformer	Experimental population (CP-FTMW)	Ab initio[a] relative energy (cm^{-1})	Predicted population (60 °C)	Effective T (K)	Transition state	Ab initio[a] transition state energy (cm^{-1})
1	0.18	212	0.40	178	1 → 7	357
2	0.44	74	0.73	130	2 → 6	303
3	1.0	0	1.0	–	3 → 5	260
4	0.023	349	0.22	133	4 → 8	252
5	0.11	115	0.61	75	5 → 3	145
6	0.0056	230	0.37	64	6 → 2	147
7	0.0051	375	0.20	102	7 → 1	194
8	–	481	–	–	8 → 4	120

[a] Zero-point energy corrected transition state barriers. A single imaginary frequency was found for each transition state. These frequencies are 258 cm^{-1}, 270 cm^{-1}, 272 cm^{-1} and 249 cm^{-1} for 5, 6, 7 and 8, respectively.

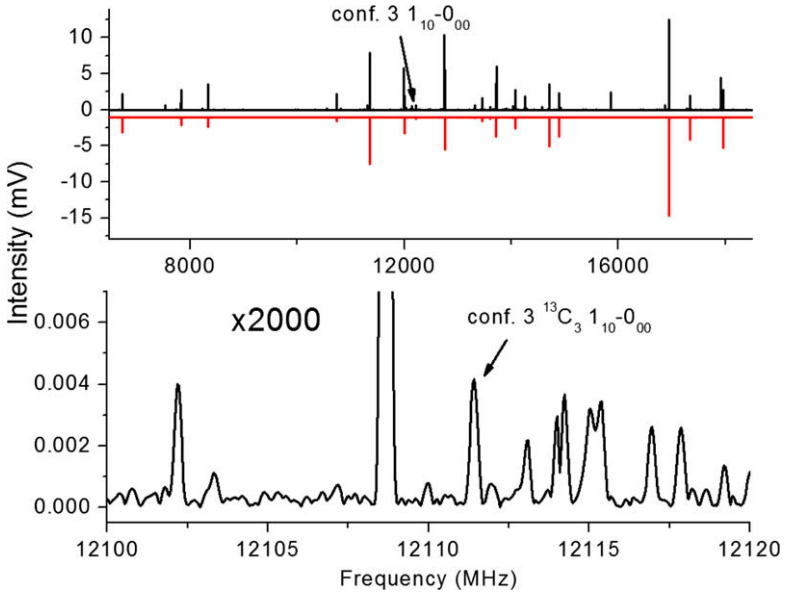

Fig. 3. The upper frame shows the full CP-FTMW spectrum after 288 000 averages, compared to a simulation (in red) of conformer 3 using the fit Hamiltonian parameters from Table 7. In the lower frame, an expanded view shows that the signal-to-noise on the strongest line (the 2_{12}–1_{01} transition of conformer 3) is in excess of 10 000:1. (For interpretation of the references to color in this figure legend, the reader is referred to the web version of this paper.)

of the four higher energy conformers of each set (i.e., 5, 6 and 7) which can lose population via this pathway, have undergone conformational cooling to a much greater extent than conformers 1, 2 and 4, which would receive population from these conformers. The extent of the cooling is even captured in the calculated zero-point-energy corrected torsional barriers given in Table 13 where the smaller degree of cooling of 7 relative to 5 and 6 may be explained by the ≈48 cm^{-1} barrier increase in 7 relative to those of 5 and 6 (≈146 cm^{-1}). This should also be contrasted with the intra-set conversion barrier from 6 to 5 of 753 cm^{-1}. Thus, these results suggest collisional cooling dynamics as an intermediate case relative to the "400 cm^{-1} barrier rule" of Ruoff et al. [27].

As a final note, the potential applications of the broadband FTMW method to thermalized gas samples in waveguides or static cells [28] would enable direct determinations of the relative energies of the conformers. Furthermore, with the high sensitivity of this method to the cooling dynamics that occur on the facile inter-conversion pathways of 1,2-propandiol and other sugar alcohols [29,30], a far-infrared variant of the population transfer method of Zwier and coworkers [31] may permit estimates of the torsional barriers. Such studies would provide full experimental determinations of the global torsional potential energy surface and rigorous tests of the ab initio theory.

8. Summary and conclusions

We have re-examined the rotational spectrum of 1,2-propanediol with both a cavity and broadband FTMW spectrometers. Caminati [8] originally reported the observation of two conformers of 1,2-propanediol, labeled conformers 1 and 2 here. Lockley et al. [18] extended the conformer set by observing conformer 3 and found it to be the lowest in energy. We have assigned four additional conformers, and confirm via theory and experiment that conformer 3 is the lowest energy form. Two other conformers, 5 and 6, are comparable in energy to the two original conformers based on MP2 ab initio calculations which are in excellent agreement with the observed molecular parameters.

9. Supplementary material

The measured spectral lines and spectral fitting for conformers 1 and 2 are given in the supplementary data. For the non-observed conformers, the ab initio structural parameters are also listed in the supplementary tables. In addition, the full CP-FTMW spectrum is available. The supplementary material can be found online on Science Direct (http://www.sciencedirect.com) and is also

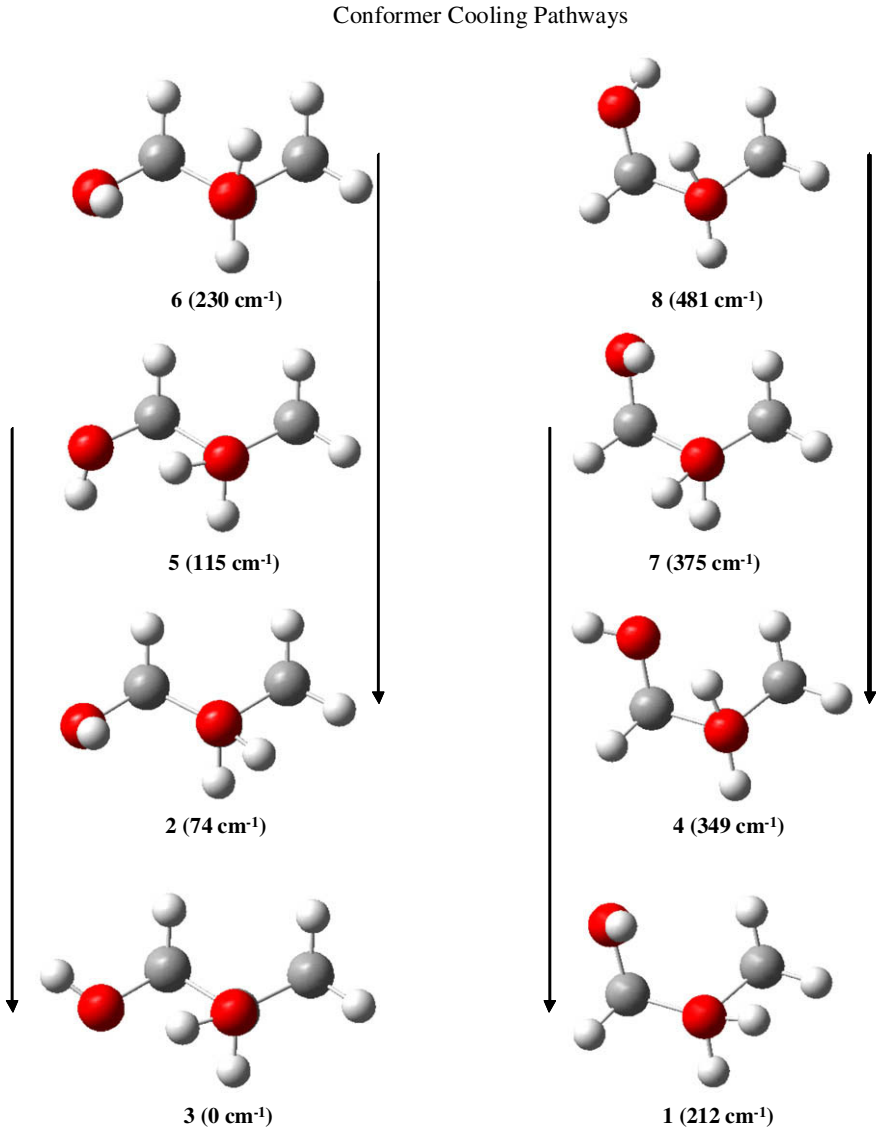

Fig. 4. The eight lowest energy conformers ordered by energy in cm^{-1} within two sets. The two sets are distinguished by whether the terminal O atom is out of the plane (left set) or in the plane (right set) of the three carbons. Within each set, the arrows indicate conformer cooling pathways involving a simple 110–120° rotation of free OH group that may explain the colder jet-cooled populations determined for three or the four higher energy conformers (See Table 13 and text for details).

available as part of the Ohio State University Molecular Spectroscopy Archives.

Acknowledgment

This was supported by the NSF Centers for Chemical Innovation through Grant 0847919.

References

[1] J.M. Hollis, F.J. Lovas, P.R. Jewell, Astrophys. J. (Lett.) 540 (2000) L107–L110.
[2] J.M. Hollis, F.J. Lovas, P.R. Jewell, L.H. Coudert, Astrophys. J. (Lett.) 571 (2002) L59–L62.
[3] G. Cooper, N. Kimmich, W. Bellsle, J. Sarinanna, K. Brabham, L. Garrel, Nature 414 (2001) 879–883.
[4] S. Vázquez, R.A. Mosquera, M.A. Rios, C. van Alsenoy, J. Mol. Struct. (Theochem) 184 (1989) 323–342.
[5] P. Pulay, Mol. Phys. 17 (1969) 299;
P. Pulay, G. Fogarasi, F. Pang, J.E. Boggs, J Am. Chem. Soc. 101 (1979) 255.
[6] C. Möller, M.S. Plesset, Phys. Rev. 46 (1934) 618;
M. Head-Grodon, J.A. Pople, M.J. Frisch, Chem. Phys. Lett. 153 (1988) 503.
[7] T.H. Dunning Jr., J. Chem. Phys. 90 (1989) 1007–1023;
D.E. Woon, T.H. Dunning Jr., J. Chem. Phys. 98 (1993) 1358–1371.
[8] W. Caminati, J. Mol. Spectrosc. 86 (1981) 193–201.
[9] T.J. Balle, W. Flygare, Rev. Sci. Instrum. 52 (1981) 33–45.
[10] F.J. Lovas, R.D. Suenram, J. Chem. Phys. 87 (1987) 2010–2020.
[11] R.D. Suenram, J.-U. Grabow, A. Zuban, I. Leonov, Rev. Sci. Instrum. 70 (1999) 2127–2135.
[12] J.-U. Grabow, W. Stahl, Z. Naturforsch. A 45 (1990) 1043–1044;
J.-U. Grabow, W. Stahl, H. Dreizler, Rev. Sci. Instrum. 67 (1996) 4072–4084.
[13] J.-U. Grabow, private communication, 2003. Available from: www.pci.uni-hannover.de/~lgpca/spectroscopy/ftmw/.

[14] G.G. Brown, B.C. Dian, K.O. Douglass, S.M. Geyer, S.T. Shipman, B.H. Pate, Rev. Sci. Instrum. 79 (2008) 53103-1–53103-13.
[15] Certain commercial products are identified in this paper in order to specify adequately the experimental or theoretical procedures. In no case does such identification imply recommendation or endorsement by the National Institute of Standards and Technology, nor does it imply that the products are necessarily the best available for the purpose.
[16] A.D. McLean, G.S. Chandler, J. Chem. Phys. 72 (1980) 5639–5648.
[17] M.J. Frisch, G.W. Trucks, H.B. Schlegel, G.E. Scuseria, M.A. Robb, J.R. Cheeseman, J.A. Montgomery, Jr., T. Vreven, K.N. Kudin, J.C. Burant, J.M. Millam, S.S. Iyengar, J. Tomasi, V. Barone, B. Mennucci, M. Cossi, G. Scalmani, N. Rega, G.A. Petersson, H. Nakatsuji, M. Hada, M. Ehara, K. Toyota, R. Fukuda, J. Hasegawa, M. Ishida, T. Nakajima, Y. Honda, O. Kitao, H. Nakai, M. Klene, X. Li, J.E. Knox, H.P. Hratchian, J.B. Cross, C. Adamo, J. Jaramillo, R. Gomperts, R.E. Stratmann, O. Yazyev, A.J. Austin, R. Cammi, C. Pomelli, J.W. Ochterski, P.Y. Ayala, K. Morokuma, G.A. Voth, P. Salvador, J.J. Dannenberg, V.G. Zakrzewski, S. Dapprich, A.D. Daniels, M.C. Strain, O. Farkas, D.K. Malick, A.D. Rabuck, K. Raghavachari, J.B. Foresman, J.V. Ortiz, Q. Cui, A.G. Baboul, S. Clifford, J. Cioslowski, B.B. Stefanov, G. Liu, A. Liashenko, P. Piskorz, I. Komaromi, R.L. Martin, D.J. Fox, T. Keith, M.A. Al-Laham, C.Y. Peng, A. Nanayakkara, M. Challacombe, P.M.W. Gill, B. Johnson, W. Chen, M.W. Wong, C. Gonzalez, and J.A. Pople, GAUSSIAN03, Revision B.04, Gaussian Inc., Pittsburgh, PA, 2003.
[18] T.J.L. Lockley, J.P.I. Hearn, A.K. King, B.J. Howard, J. Mol. Struct. 612 (2002) 199–206.
[19] L.H. Coudert, F.J. Lovas, R.D. Suenram, J.T. Hougen, J. Chem. Phys. 87 (1987) 6290–6299.
[20] J.M.L.J. Reinartz, A. Dymanus, Chem. Phys. Lett. 24 (1974) 346–351.
[21] B.N. Taylor, C.E. Kuyatt, NIST Tech. Note 1297 (1994) 1–20. The publication may be downloaded from http://physics.nist.gov/Pubs/guidelines/contents.html.
[22] See http://www.cv.nrao.edu/aremijan/PRIMOS/ for more information on the project.
[23] B.L. Ulich, R.W. Haas, Astrophy. J. Suppl. 30 (1976) 247–258.
[24] J.M. Hollis, P.R. Jewell, F.J. Lovas, A. Remijan, Astrophys. J. 613 (2004) L45–L48.
[25] J.M. Hollis, Proc. IAU Symp. No. 231 (2006) 227–236.
[26] R.D. Suenram, G.Yu. Golubiatnikov, I.I. Leonov, J.T. Hougen, J. Ortigoso, I. Kleiner, G.T. Fraser, J. Mol. Spectrosc. 208 (2001) 188–193.
[27] R.S. Ruoff, T.D. Klots, T. Emilsson, H.S. Gutowsky, J. Chem. Phys. 93 (1990) 3142–3150.
[28] S.T. Shipman, private communication 2009.
[29] V.V. Iluyshin, R.A. Motiyenko, F.J. Lovas, D.F. Plusquellic, J. Mol. Spectrosc. 251 (2008) 129–137.
[30] F.J. Lovas, D.F. Plusquellic, B.H. Pate, J.L. Neill, M.T. Muckle, A.J. Remijan, private communication 2009.
[31] B.C. Dian, J.R. Clarkson, T.S. Zwier, Science 303 (2004) 1169–1173.